

## Multidimensional Volumetric Imaging of Pulmonary Infiltrates for Measuring Therapeutic Response to Antifungal Therapy in Experimental Invasive Pulmonary Aspergillosis

Vidmantas Petraitis,<sup>1,2</sup> Ruta Petraitiene,<sup>1,2</sup> Jeffrey Solomon,<sup>3</sup> Amy M. Kelaher,<sup>1</sup> Heidi A. Murray,<sup>1</sup> Christine Mya-San,<sup>1</sup> Avi K. Bhandary,<sup>1</sup> Tin Sein,<sup>1</sup> Nilo A. Avila,<sup>4</sup> Algidas Basevicius,<sup>5</sup> John Bacher,<sup>6</sup> and Thomas J. Walsh<sup>1\*</sup>

*Immunocompromised Host Section, Pediatric Oncology Branch, National Cancer Institute, National Institutes of Health, Bethesda, Maryland<sup>1</sup>; SAIC-Frederick, Inc., Frederick, Maryland<sup>2</sup>; Medical Numerics, Inc., Sterling, Virginia<sup>3</sup>; Department of Radiology, Warren Grant Magnuson Clinical Center, National Institutes of Health, Bethesda, Maryland<sup>4</sup>; Departments of Radiology, Kaunas University of Medicine, Kaunas, Lithuania<sup>5</sup>; and Division of Veterinary Resources, Office of Research Services, National Institutes of Health, Bethesda, Maryland<sup>6</sup>*

Received 11 August 2005/Returned for modification 28 November 2005/Accepted 6 February 2006

**Pulmonary infiltrates in neutropenic hosts with invasive pulmonary aspergillosis are caused by vascular invasion, hemorrhagic infarction, and tissue necrosis. Monitoring the dynamics of pulmonary infiltrates of invasive aspergillosis is an important tool for assessing response to antifungal therapy. We, therefore, introduced a multidimensional volumetric imaging (MDVI) method for analysis of the response of the volume of pulmonary infiltrates over time to antifungal therapy in experimental invasive pulmonary aspergillosis (IPA) in persistently neutropenic rabbits. We developed a semiautomatic method to measure the volume of lung lesions, which was implemented as an extension of the MEDx visualization and analysis software using ultrafast computerized tomography (UFCT). Volumetric infiltrate measures were compared with UFCT reading, histopathological resolution of lesions, microbiological clearance of *Aspergillus fumigatus*, and galactomannan index (GMI). We also studied the MDVI method for consistency and reproducibility in comparison to UFCT. Treatment groups consisted of deoxycholate amphotericin B (DAMB) at 0.5 or 1 mg/kg of body weight/day and untreated controls (UC). Therapeutic monitoring of pulmonary infiltrates using MDVI demonstrated a significant decrease in the infiltrate volume in DAMB-treated rabbits in comparison to UC ( $P \leq 0.001$ ). Volumetric data by MDVI correlated with conventional CT pulmonary scores ( $r = 0.83$ ,  $P \leq 0.001$ ). These results correlated with validated biological endpoints: pulmonary infarct scores ( $r = 0.85$ ,  $P \leq 0.001$ ), lung weights ( $r = 0.76$ ,  $P \leq 0.01$ ), residual fungal burden ( $r = 0.65$ ,  $P \leq 0.05$ ), and GMI ( $r = 0.78$ ,  $P \leq 0.01$ ). MDVI correlated with key biological markers, improved the objectivity of radiological assessment of therapeutic response to antifungal therapy, and warrants evaluation for monitoring therapeutic response in immunocompromised patients with invasive aspergillosis.**

Invasive pulmonary aspergillosis (IPA) is an important cause of morbidity and mortality in immunocompromised patients (1, 4, 8, 10, 12, 15, 24). Despite recent advances in the therapy of invasive pulmonary aspergillosis, more objective and consistent systems are needed to improve timely treatment and monitoring of therapeutic response by computerized tomography (CT) imaging. In recent years, notable progress has been made in three-dimensional imaging and volumetric measures of tumor size (20). Recent advances in CT technology and image processing permit accurate measurement of volumetric tumor burden. Radiological evaluation of tumor size using volumetric measures has been used in clinical trials of anticancer pharmaceuticals and has become a surrogate marker of therapeutic response (19).

The usage of ultrafast CT (UFCT) for early detection and therapeutic monitoring of invasive pulmonary aspergillosis has been studied in neutropenic patients (2, 3, 5, 9, 11, 27) and in

neutropenic animals (16, 17, 18, 26). The pulmonary infiltrates of invasive pulmonary aspergillosis in neutropenic hosts are the direct result of organism-mediated pulmonary injury caused by angioinvasion, hemorrhage, and necrosis. Pulmonary infarct scores and lung weights are a direct measurement of this organism-mediated pulmonary injury. With the recent introduction of computerized methods, determination of the volumes of pulmonary infiltrates has now become possible. Therapeutic monitoring of pulmonary infiltrates of invasive pulmonary aspergillosis may be a useful tool for assessing antifungal therapy and dosage regimens. Understanding the correlation between the dynamics of infiltrate volume and key outcome variables, including microbiological response, resolution of pathologically defined lesions, and antigenemia, could provide valuable future clinical applications. To our knowledge, there are no published reports describing volumetric measures of pulmonary infiltrates of invasive pulmonary aspergillosis or other forms of infectious pneumonia in immunocompromised patients. We, therefore, developed and introduced a multidimensional volumetric imaging (MDVI) method to assess the response to antifungal therapy of IPA in experimental pulmonary aspergillosis. We further studied the accu-

\* Corresponding author. Mailing address: Immunocompromised Host Section, Pediatric Oncology Branch, National Cancer Institute, Building 10, CRC, Rm. 1W-5740, 10 Center Dr., MSC 1100, Bethesda, MD 20892-1100. Phone: (301) 496-7103. Fax: (301) 480-2308. E-mail: walshjt@mail.nih.gov.

racy and reproducibility of MDVI in comparison to conventional assessments of UFCT scans.

#### MATERIALS AND METHODS

**Organisms.** NIH isolate *Aspergillus fumigatus* 4215 (ATCC no. MYA-1163), obtained from a patient with a fatal case of pulmonary aspergillosis, was used in all experiments. MICs against *A. fumigatus* were determined according to CLSI (formerly NCCLS) standard M38-A microdilution methods (6, 13). The MIC of amphotericin B against *A. fumigatus* 4215 was 1.0  $\mu\text{g/ml}$  in RPMI 1640 (Bio-Whittaker, Walkersville, MD).

**Animals.** Healthy female New Zealand White rabbits (Hazleton Research Products, Inc., Denver, PA) weighing 2.6 to 3.5 kg at the time of endotracheal inoculation were used in all experiments. All rabbits were monitored under humane care and use standards in facilities accredited by the Association for Assessment and Accreditation of Laboratory Animal Care International and according to National Institutes of Health guidelines for animal care in fulfillment of guidelines of the National Research Council (14) and under approval by the Animal Care and Use Committee of the National Cancer Institute. A total of 15 rabbits were used for all experiments. Vascular access was established in each rabbit as previously described (25). Rabbits were euthanized by intravenous (i.v.) administration of pentobarbital (65 mg of pentobarbital sodium/kg of body weight) given at the end of each experiment, 24 h after the administration of the last dose of study drug. (Note that pentobarbital sodium was in the form of 0.5 ml of Beuthanasia-D special euthanasia solution [Schering-Plough Animal Health Corp., Union, NJ].)

**Inoculation.** Pulmonary aspergillosis was established as described previously (7). The concentration was adjusted in order to give each rabbit a predetermined inoculum of  $1.0 \times 10^8$  to  $1.25 \times 10^8$  conidia of *A. fumigatus* in a volume of 250 to 350  $\mu\text{l}$ . The concentrations of the inocula were confirmed by quantitative cultures of serial dilutions inoculated onto Sabouraud glucose agar.

Inoculation was performed on day 2 of the experiments, while the rabbits were under general anesthesia. The *A. fumigatus* inoculum was administered endotracheally under direct visualization with a tuberculin syringe attached to a 5 1/4-in. 16-gauge Teflon catheter (Becton Dickinson Infusion Therapy Systems, Inc., Sandy, UT).

**Immunosuppression and maintenance of neutropenia.** Immunosuppression and neutropenia were established, as previously described (16), with i.v. treatment with cytarabine (Ara-C) (Cytosar-U; Pharmacia & Upjohn, Kalamazoo, MI) 1 day before endotracheal inoculation of the animals by an initial course of 525 mg of Ara-C per  $\text{m}^2$  for 5 consecutive days and methylprednisolone (Abbott Laboratories, North Chicago, IL) at a dose of 5 mg/kg of body weight/day administered on days 1 and 2. A maintenance dose of 484 mg of Ara-C per  $\text{m}^2$  was administered for 4 additional days on days 8, 9, 13, and 14 of the experiment. Total leukocyte counts and the percentages of granulocytes were monitored twice weekly with a Beckman Coulter Z1 Dual counter (Beckman Coulter, Inc., Miami, FL) and by peripheral blood smears and differential counts, respectively. Cefazidime (75 mg/kg given i.v. twice daily; Glaxo, Inc., Research Triangle Park, NC), gentamicin (5 mg/kg given i.v. every other day; Elkins-Sinn, Inc., Cherry Hill, NJ), and vancomycin (15 mg/kg given i.v. daily; Abbott Laboratories, North Chicago, IL) were administered from day 4 of immunosuppression until study completion to prevent opportunistic bacterial infections during neutropenia. In order to prevent antibiotic-associated diarrhea due to *Clostridium spiroforme*, all rabbits continuously received 50 mg of vancomycin per liter of drinking water.

**Antifungal compounds and treatment regimens.** Rabbits were grouped to receive desoxycholate amphotericin B at 0.5 mg/kg/day (DAMB0.5) or 1 mg/kg/day (DAMB1) for treatment of established invasive pulmonary aspergillosis or were grouped as untreated controls (UC). Antifungal therapy was administered for 12 days starting 24 h after endotracheal inoculation of *A. fumigatus* conidia.

**Outcome variables.** The following panel of outcome variables was used to assess antifungal efficacy: multidimensional infiltrate volume ( $\text{mm}^3$ ) UFCT, pulmonary infarct score, lung weight, residual fungal burden ( $\log [\text{CFU/g}]$ ), and galactomannan antigenemia. Pulmonary infarct score and lung weight are measures of organism-mediated pulmonary injury.

**UFCT.** Serial CT scans of the lungs were performed during all experiments as previously described (26). Briefly, rabbits were sedated with ketamine and xylazine and then placed prone, headfirst, on the scanning couch. CT was performed with the ultrafast electron beam CT scanner (model CE 0459, HiSpeed CT/i; GE Medical Systems, Milwaukee, WI). Using the high-resolution, table-incremented, volume acquisition mode, we performed 1.25-mm-thick ultrafast CT scans every 4 s. A small scan circle and a 9.6-cm-diameter reconstruction circle with a matrix of 512 by 512 were used, which resulted in a pixel size of less than 1 mm. Scan

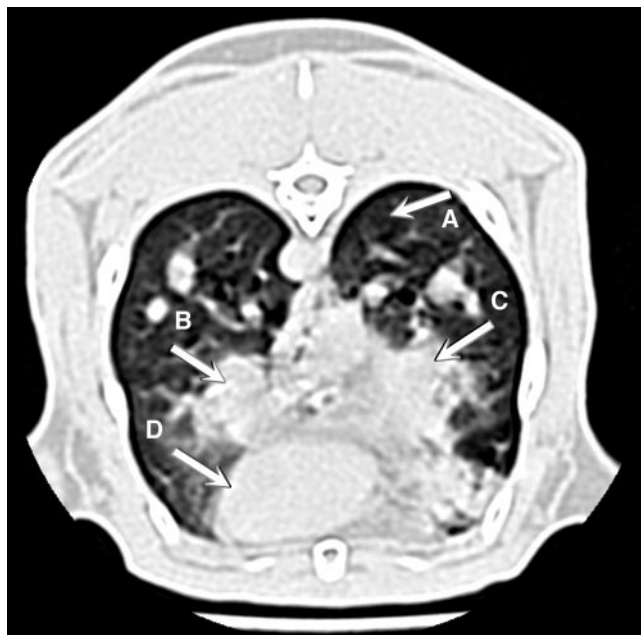


FIG. 1. Two-dimensional computerized tomography image of rabbit lung with invasive pulmonary aspergillosis. Arrows point to (A) normal lung tissue, (B) nodular pulmonary infiltrate, (C) bronchopneumonia with irregular boundaries caused by invasive pulmonary aspergillosis involving the right middle lobe and right lower lobe, and (D) the contour of the heart.

parameters were 80 kV, 120 mA, and scan duration was 0.8 s. In virtually all cases, 60 slices were sufficient to scan the entire thorax of the rabbit. Images were photographed using lung windows with a level of  $-600$  Hounsfield units and a width of 1,800 Hounsfield units. The data were processed to generate two-dimensional images, as depicted in Fig. 1.

**Multidimensional pulmonary infiltrate volume measures.** We developed a semiautomatic method to measure the volume of lung lesions. This method was implemented as an extension of the MEDx visualization and analysis software (Medical Numerics, Inc., Sterling, VA). An example of the CT image used in the analysis software to generate a volume measurement is presented in Fig. 2.

The steps used in the technique are described below. A point is placed within the lung on each CT section. For each CT section, we then performed the following steps. (i) We performed seeded region growing with an inclusion threshold range of  $(-1,023$  to  $775)$  to segment the lung. (ii) A contour of the segmented lung boundary was automatically created. (iii) If necessary, we selected the option to semiautomatically exclude non-lung tissue or include non-segmented lung tissue and to reperform region growing. (iv) If necessary, we made fine manual adjustments of the lung boundary contour. (v) We computed the area of all pixels inside the lung boundary contour that are above a threshold of  $-500$  Hounsfield units. This is the lung lesion area. We then determined the sum of the lesion areas from all relevant CT sections and multiplied it by the slice thickness. This is the total lesion volume.

We implemented a common strategy of first segmenting the lung image and then looking inside the lung tissue for lesions. The use of an automatic method to segment the lung, such as seeded region growing, provides for a robust technique with less inter/intraoperator variability than manual tracing. The threshold range  $(-1,023$  to  $775)$  was determined empirically. If it is necessary to include/exclude tissue that was not properly segmented in the region-growing step, an option exists for the operator to trace the targeted tissue to include/exclude. For inclusion, the pixel values within the targeted tissue will be modified to be within the threshold range. For exclusion, the pixel values will be modified to be outside the threshold range. The region-growing algorithm is again performed, and the targeted tissue is now included/excluded as desired. The threshold value of  $-500$  Hounsfield units for lesion determination was based on previous literature (21, 22) and empirical evidence. Selecting a threshold value of  $-500$  Hounsfield units excludes the air in the lungs but might include blood vessels, which have similar density to the lung lesions. Inclusion of these small

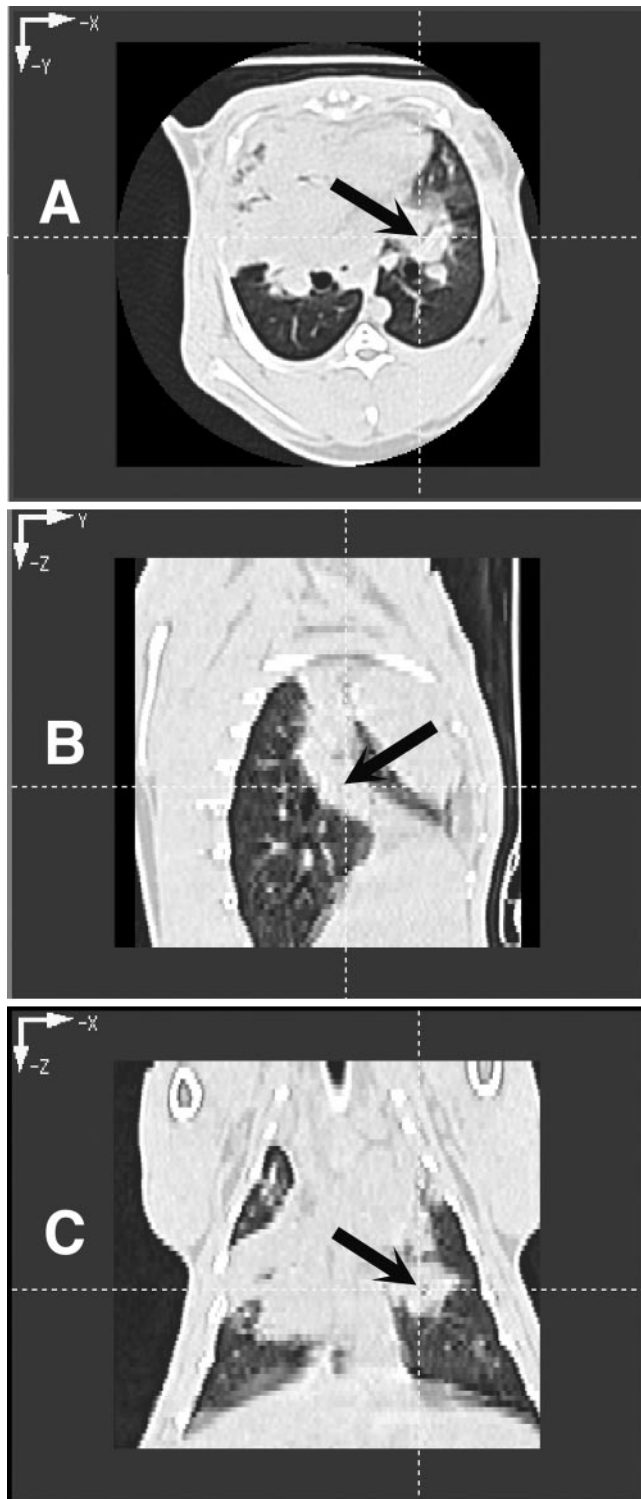


FIG. 2. CT images of rabbit lung in three planes. (A and B) Transverse plane depicting pulmonary infiltrates in both lower lobes (A) and section of lungs depicting pulmonary infiltrates due to invasive pulmonary aspergillosis (B). Note that the pulmonary infiltrate when viewed in the sagittal plane depicts a column of infiltrate, which on transverse section appeared to be spherical. (C) Coronal image plane of rabbit lungs with experimental invasive pulmonary aspergillosis depicting irregularly contoured pulmonary infiltrates.

vessels may reduce the sensitivity of detecting a lesion volume change over time. Representative maximum intensity projections from untreated control and DAMB-treated rabbits are depicted in Fig. 3.

**Postmortem examination, pulmonary lesion scores, and lung weights.** The entire heart-lung block was carefully resected at autopsy. Postmortem examination of the lungs was performed as previously described (16).

**Fungal cultures.** Lung tissue from each rabbit was sampled and cultured by a standard excision of tissue from each lobe (16). Each fragment was individually placed in a sterile polyethylene bag (Tekmar Corp., Cincinnati, OH), weighed, and homogenized with sterile saline for 30 s per tissue sample (Stomacher 80; Tekmar Corp., Cincinnati, OH) (28). The number of CFU of *A. fumigatus* was counted and recorded for each lobe, and the CFU per gram were calculated. A finding of one colony of *A. fumigatus* was considered positive.

**Galactomannan assay.** Blood was collected every other day from each rabbit for determination of serum galactomannan levels. Serum galactomannan levels were determined by using the Platelia *Aspergillus* enzyme immunoassay (EIA) (Bio-Rad Laboratories, Redmond, WA), a one-stage immunoenzymatic sandwich microplate assay method, which was performed according to the manufacturer's directions (Platelia *Aspergillus* EIA for immunoenzymatic detection of galactomannan antigen of *Aspergillus* in serum; Bio-Rad, Marnes la Coquette, France). The assay uses rat monoclonal antibody EB-A2, which is directed against *Aspergillus* galactomannan (23). The monoclonal antibody is used to sensitize the wells of the microplate and to bind the antigen. Peroxidase-linked monoclonal rat antibody is used as the detector antibody. The optical absorbencies of specimens and controls are determined by using a microplate spectrophotometer equipped with 450- and 620-nm filters (Titertek Multiscan MMC/340; Titertek, Huntsville, AL).

Enzyme immunoassay data were expressed as the serum galactomannan index (GMI) plotted over time. The GMI for each test serum is equal to the optical density of a sample divided by the optical density of a threshold serum provided in the test kit. Sera with GMIs less than 0.5 were considered negative. Serial serum galactomannan levels were plotted over time of administration of anti-fungal compound.

**Statistical analysis.** Comparisons between groups were performed by using the Kruskal-Wallis test (nonparametric analysis of variance), the Mann-Whitney U test, or the Spearman rank correlation coefficient, as appropriate. A two-tailed *P* value of <0.05 was considered to be statistically significant. Values are expressed as means and standard errors of the means.

## RESULTS

There was a significant dose-dependent decrease in volume of pulmonary infiltrates in DAMB-treated rabbits in comparison to that of UC ( $P \leq 0.001$ ) (Fig. 4A). During the first 4 days of therapy, there was an increase in the volume of pulmonary infiltrates in all three groups. However, the volume was lower in a dose-dependent manner in treatment groups. After day 4 of therapy, there was a significant decrease of pulmonary infiltrate volume in DAMB0.5- and DAMB1-treated rabbits, while the volume of pulmonary infiltrates in UC sharply increased. The patterns of pulmonary infiltrates, using two-dimensional scoring, over time (Fig. 4B), were similar to those of the pulmonary infiltrate volume. The dynamics of the pulmonary infiltrate volume correlated with changes in the pulmonary infiltrate score measured using conventional UFCT ( $r = 0.83$ ,  $P \leq 0.001$ ) (Fig. 4C).

There also was a strong correlation between infiltrate volume and validated key outcome variables. The volume of pulmonary infiltrates correlated in a dose-dependent manner with changes of organism-mediated pulmonary injury as measured by pulmonary infarct score ( $r = 0.85$ ,  $P \leq 0.001$ ) and total lung weights ( $r = 0.76$ ,  $P \leq 0.01$ ) (Fig. 5A and B). In addition, a good correlation was observed between infiltrate volume and residual fungal burden, as measured by log CFU/g ( $r = 0.65$ ,  $P \leq 0.05$ ) (Fig. 5C). There was a strong correlation between the volume of pulmonary infiltrates and galactomannan anti-

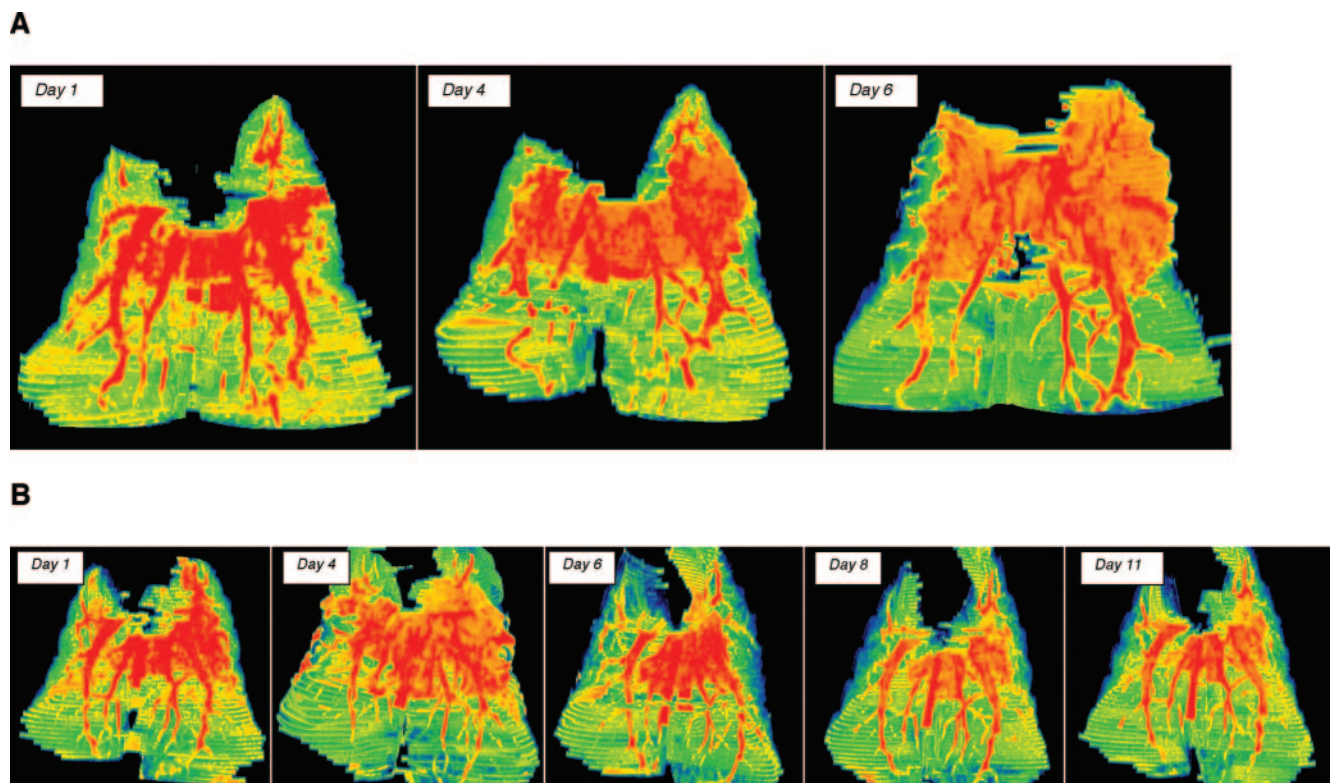


FIG. 3. Pseudocolor images of multidimensional reconstruction of pulmonary infiltrates of experimental aspergillosis. (A) Pseudocolor images of pulmonary infiltrates due to experimental pulmonary aspergillosis of untreated controls demonstrate progressive lesions expanding in three dimensions in predominantly the upper lobes. Day 1 images demonstrate highly dense infiltrate in association with early pulmonary hemorrhage; as the lesion expands, there is an increasing level of infection with progressive blood vessel involvement due to angioinvasion. By day 6, the lesions have expanded and have changed in density, reflecting the development of pulmonary infarcts, as well as disruptive blood vessels in association with angioinvasion. (B) Multidimensional pseudocolor reconstruction of experimental pulmonary aspergillosis in a rabbit treated with deoxycholate amphotericin B. The reconstructed CT image on day 1 depicts early pulmonary hemorrhage and expanding infiltrates. However, by day 4 infiltrates have stabilized and have tended to diminish. There is early evidence of blood vessel invasion. By day 6, there are substantial resolution of infiltrates and an apparent increase in vessels, which continue into day 8 and finally day 11. By day 11, pulmonary infiltrates have virtually resolved and the blood vessels have returned to a normal anatomic structure.

genemia as a surrogate marker of antifungal therapeutic response ( $r = 0.78$ ,  $P \leq 0.01$ ) (Fig. 5D).

## DISCUSSION

This study introduces a new multidimensional volumetric CT imaging system for the therapeutic monitoring of invasive pulmonary aspergillosis. The system becomes multidimensional with a fourth dimension of time that projects the changes in volume of pulmonary infiltrates. Our study demonstrated that the volume of pulmonary infiltrates produced by invasive aspergillosis increases over the course of time and correlates strongly with the evolution of histologically documented pulmonary infarcts. When antifungal therapy is instituted, the pulmonary infiltrate volume declines over time in parallel with the histologically documented pulmonary infarct score. The multidimensional imaging system for monitoring pulmonary infiltrates also correlates with other biological variables of lung weight, residual fungal burden (log CFU/g), and the serum GMI.

The pulmonary infiltrates on CT scan images represent pulmonary injury caused by hemorrhagic infarction. Pulmonary infarcts and total lung weights are direct indicators of pulmonary injury. Their correlation with three-dimensional CT infil-

trate volume is somewhat stronger ( $r = 0.85$  and  $r = 0.76$ , respectively) than that of residual fungal burden ( $r = 0.65$ ). The lower correlation coefficient is a reflection of variations in regional sampling from individual lobes. Although standard lung sections are routinely obtained postmortem, there is a greater degree of variation than to that of serum galactomannan, which reflects the total residual fungal burden in both lungs.

Monitoring of therapeutic response by conventional analysis of CT scans requires examination of individual panels in an attempt to make an assessment of changing size based on two-dimensional images. These assessments are often subjective and may vary depending upon the inconsistencies of images of different planes of pulmonary lesions. This analysis becomes more complicated in the setting of complicated pulmonary infiltrates and multiple nodules. Inconsistencies may also occur across lesions, in which some lesions may appear to expand and one or more may improve. Alternatively, some lesions may demonstrate a decrease in size, suggesting an improved response, while one or more other lesions may simultaneously appear to increase in size, suggesting progression.

A more objective global assessment of therapeutic response

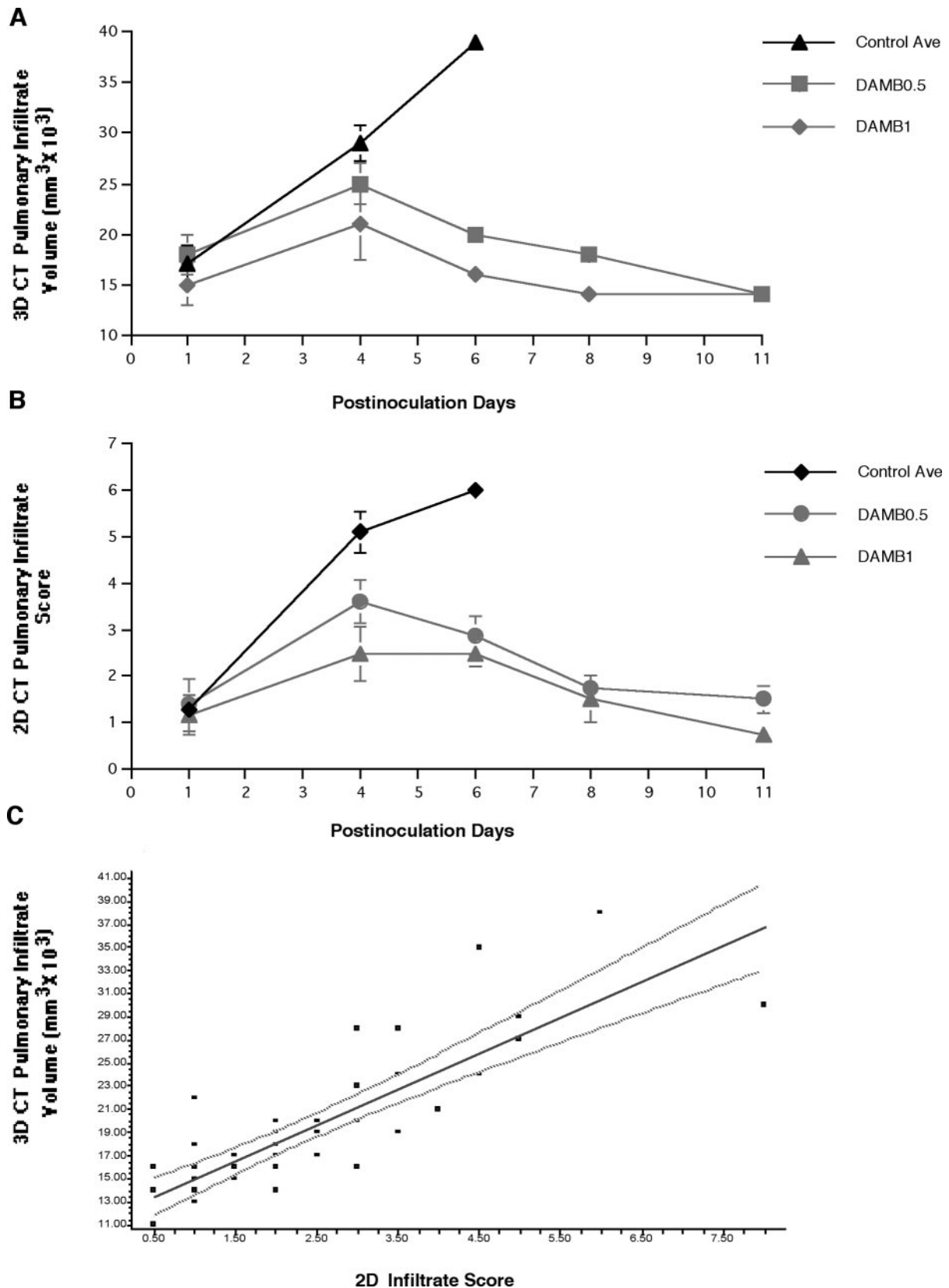


FIG. 4. Time versus three-dimensional (3D) CT pulmonary infiltrate volume (A) and CT infiltrate score determined by conventional two-dimensional (2D) CT scan analysis (B) depict similar patterns of lesions in untreated controls and response to deoxycholate amphotericin B therapy at 0.5 and 1 mg/kg/day (DAMB0.5 and DAMB1, respectively). Panel C depicts the correlation between CT pulmonary infiltrate volume determined by three-dimensional analysis and the infiltrate score determined by two-dimensional analysis. A strong correlation ( $r = 0.83$ ,  $P \leq 0.001$ ) was found between the data from these two imaging analysis techniques.

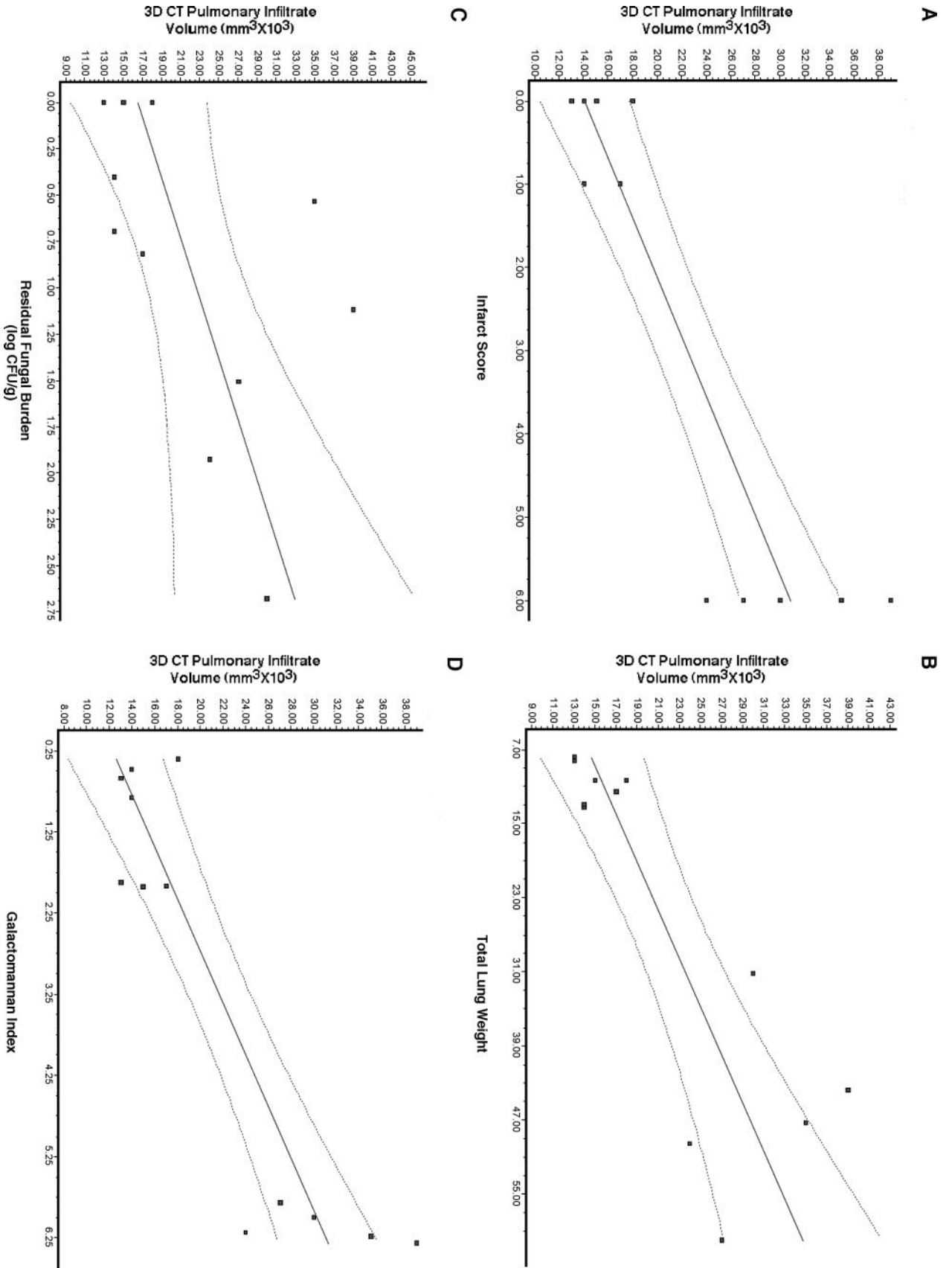


FIG. 5. Pearson's correlation analysis between three-dimensional (3D) CT pulmonary infiltrate volume and pulmonary infarct scores (A), lung weights (B), residual fungal burden ( $\log \text{CFU/g}$ ) (C), and galactomannan index (D). Correlations were found for all variables: infarct score ( $r = 0.85$ ,  $P \leq 0.001$ ), total lung weights ( $r = 0.76$ ,  $P \leq 0.01$ ), residual fungal burden ( $\log \text{CFU/g}$ ;  $r = 0.65$ ,  $P \leq 0.05$ ), and galactomannan index ( $r = 0.78$ ,  $P \leq 0.01$ ).

by CT scan may be achieved using a total volume rather than a two-dimensional image across complicated infiltrates or multiple-difference nodules. The MDVI methodology allows for computerized reconstruction of the pulmonary infiltrate to yield a three-dimensional volume. This more objective unit of a total infiltrate volume adjusts for artifactual changes in the plane of scanning for pulmonary infiltrates. By comparing an individual number, representing a three-dimensional volume of infiltrates, a more consistent comparison of scans can be achieved over time.

Certainly the use of MDVI does not preclude the need for visual inspection of the characteristics of each pulmonary infiltrate. We propose that the MDVI system could be applied to therapeutic monitoring of invasive pulmonary aspergillosis and possibly other pneumonic infiltrates in humans as an adjunct to assessment of response.

Multidimensional imaging has been successfully used in patients for measurements of therapeutic response of tumors to antineoplastic therapy (19, 20). Sohaib et al. (20) evaluated a helical CT scan for assessing tumor response by standard criteria (changes in two-dimensional cross-sectional areas) in comparison to three-dimensional measurements. The three-dimensional measurements for monitoring the therapeutic response to tumors were found to be accurate and reproducible, particularly for larger tumor volumes. Prasad et al. (19) also employed volumetric techniques to measure the response of 38 patients with liver metastases from breast cancer in comparison to unidimensional and bidimensional measurement techniques. The use of volumetric measurement revealed that most metastatic lesions were predominantly spherical with well-defined margins. Volumetric measurements demonstrated that different results may occur in patients with tumor lesions that were asymmetrical during tumor growth or shrinkage. The parallels of these studies of therapeutic response to antineoplastic therapy and those of pulmonary infiltrates of antifungal therapy suggest that volumetric measurement of therapeutic response of pulmonary infiltrates of invasive pulmonary aspergillosis may provide an important tool for assessing the efficacy of antifungal therapy in clinical research and in patient care. The MDVI method could be particularly useful in patients with IPA (or other mold pneumonias) in whom serodiagnosis is not positive (galactomannan index,  $\beta$ -D-glucan, and others).

Multidimensional volumetric imaging also may be applicable to the study of other experimental pneumonias. Real-time imaging of experimental pneumonic infiltrates may allow for closer clinical simulation if the same animal is used as its own control. This potentially would reduce the number of animals needed for a study and may obviate the need to sacrifice the experimental animals. The advanced imaging MEDx software and enhancements for pulmonary imaging used in this study are readily available through Medical Numerics, Inc., Sterling, VA, for such applications.

Multidimensional imaging techniques that reconstruct the pulmonary infiltrates revealed that these infiltrates may be irregular in conformation and that such irregularity is not apparent in conventional two-dimensional images (Fig. 1). Changes in the position of the scan may result in inaccurate assessment of the geometry of the lesion, as well as therapeutic response in these irregularly contoured pulmonary infiltrates.

Thus, MDVI offers a new strategy of assessment of therapeutic response of pulmonary infiltrates in experimental pulmonary aspergillosis and infectious pneumonias in laboratory animals. Further studies of imaging algorithms in patients with IPA and fungal pneumonias are warranted for MDVI assessment of therapeutic response in clinical trials and patient care.

#### ACKNOWLEDGMENT

This research was supported by the Intramural Research Program of the National Cancer Institute, Division of Veterinary Resources, and Clinical Center.

#### REFERENCES

- Anaissie, E. 1992. Opportunistic mycoses in the immunocompromised host: experience at a cancer center and review. *Clin. Infect. Dis.* **14**(Suppl. 1):S43–S53.
- Caillot, D. 2003. Intravenous itraconazole followed by oral itraconazole for the treatment of amphotericin-B-refractory invasive pulmonary aspergillosis. *Acta Haematol.* **109**:111–118.
- Caillot, D., J. F. Couaillier, A. Bernard, O. Casasnovas, D. W. Denning, L. Mannone, J. Lopez, G. Couillault, F. Piard, O. Vagner, and H. Guy. 2001. Increasing volume and changing characteristics of invasive pulmonary aspergillosis on sequential thoracic computed tomography scans in patients with neutropenia. *J. Clin. Oncol.* **19**:253–259.
- Denning, D. W. 2001. Chronic forms of pulmonary aspergillosis. *Clin. Microbiol. Infect.* **7**(Suppl. 2):25–31.
- Denning, D. W., P. Ribaud, N. Milpied, D. Caillot, R. Herbrecht, E. Thiel, A. Haas, M. Ruhnke, and H. Lode. 2002. Efficacy and safety of voriconazole in the treatment of acute invasive aspergillosis. *Clin. Infect. Dis.* **34**:563–571.
- Espinel-Ingroff, A., M. Bartlett, R. Bowden, N. X. Chin, C. Cooper, Jr., A. Fothergill, M. R. McGinnis, P. Menezes, S. A. Messer, P. W. Nelson, F. C. Odds, L. Pasarell, J. Peter, M. A. Pfaller, J. H. Rex, M. G. Rinaldi, G. S. Shankland, T. J. Walsh, and I. Weitzman. 1997. Multicenter evaluation of proposed standardized procedure for antifungal susceptibility testing of filamentous fungi. *J. Clin. Microbiol.* **35**:139–143.
- Francis, P., J. W. Lee, A. Hoffman, J. Peter, A. Francesconi, J. Bacher, J. Shelhamer, P. A. Pizzo, and T. J. Walsh. 1994. Efficacy of unilamellar liposomal amphotericin B in treatment of pulmonary aspergillosis in persistently granulocytopenic rabbits: the potential role of bronchoalveolar D-mannitol and serum galactomannan as markers of infection. *J. Infect. Dis.* **169**:356–368.
- Groll, A. H., P. M. Shah, C. Mentzel, M. Schneider, G. Just-Nuebling, and K. Huebner. 1996. Trends in the postmortem epidemiology of invasive fungal infections at a university hospital. *J. Infect.* **33**:23–32.
- Herbrecht, R., D. W. Denning, T. F. Patterson, J. E. Bennett, R. E. Greene, J. W. Oestmann, W. V. Kern, K. A. Marr, P. Ribaud, O. Lortholary, R. Sylvester, R. H. Rubin, J. R. Wingard, P. Stark, C. Durand, D. Caillot, E. Thiel, P. H. Chandrasekar, M. R. Hodges, H. T. Schlamme, P. F. Troke, B. de Pauw, et al. 2002. Voriconazole versus amphotericin B for primary therapy of invasive aspergillosis. *N. Engl. J. Med.* **347**:408–415.
- Latge, J.-P. 1999. *Aspergillus fumigatus* and aspergillosis. *Clin. Microbiol. Rev.* **12**:310–350.
- Maertens, J., I. Raad, G. Petrikos, M. Boogaerts, D. Selleslag, F. B. Petersen, C. A. Sable, N. A. Kartsonis, A. Ngai, A. Taylor, T. F. Patterson, D. W. Denning, T. J. Walsh, et al. 2004. Efficacy and safety of caspofungin for treatment of invasive aspergillosis in patients refractory to or intolerant of conventional antifungal therapy. *Clin. Infect. Dis.* **39**:1563–1571.
- Marr, K. A., T. Patterson, and D. Denning. 2002. Aspergillosis. Pathogenesis, clinical manifestations, and therapy. *Infect. Dis. Clin. N. Am.* **16**:875–894.
- National Committee for Clinical Laboratory Standards. 2000. Reference method for broth dilution antifungal susceptibility testing of conidium-forming filamentous fungi. Approved standard M38-A. National Committee for Clinical Laboratory Standards, Wayne, Pa.
- National Research Council Committee on the Care and Use of Laboratory Animals of the Institute of Laboratory Animal Resources. Commission on Life Sciences. 1996. Guide for the care and use of laboratory animals. National Academy Press, Washington, D.C.
- Pannuti, C., R. Gingrich, M. A. Pfaller, C. Kao, and R. P. Wenzel. 1992. Nosocomial pneumonia in patients having bone marrow transplant. Attributable mortality and risk factors. *Cancer* **69**:2653–2662.
- Petraitiene, R., V. Petraitis, A. H. Groll, T. Sein, R. L. Schauffele, A. Francesconi, J. Bacher, N. A. Avila, and T. J. Walsh. 2002. Antifungal efficacy of caspofungin (MK-0991) in experimental pulmonary aspergillosis in persistently neutropenic rabbits: pharmacokinetics, drug disposition, and relationship to galactomannan antigenemia. *Antimicrob. Agents Chemother.* **46**:12–23.
- Petraitiene, R., V. Petraitis, A. H. Groll, T. Sein, S. Piscitelli, M. Candelario, A. Field-Ridley, N. Avila, J. Bacher, and T. J. Walsh. 2001. Antifungal activity

- and pharmacokinetics of posaconazole (SCH 56592) in treatment and prevention of experimental invasive pulmonary aspergillosis: correlation with galactomannan antigenemia. *Antimicrob. Agents Chemother.* **45**:857–869.
18. **Petratis, V., R. Petraitiene, A. A. Sarafandi, A. M. Kelaher, C. A. Lyman, H. E. Casler, T. Sein, A. H. Groll, J. Bacher, N. A. Avila, and T. J. Walsh.** 2003. Combination therapy in treatment of experimental pulmonary aspergillosis: synergistic interaction between an antifungal triazole and an echinocandin. *J. Infect. Dis.* **187**:1834–1843.
  19. **Prasad, S. R., K. S. Jhaveri, S. Saini, P. F. Hahn, E. F. Halpern, and J. E. Sumner.** 2002. CT tumor measurement for therapeutic response assessment: comparison of unidimensional, bidimensional, and volumetric techniques initial observations. *Radiology* **225**:416–419.
  20. **Sohaib, S. A., B. Turner, J. A. Hanson, M. Farquharson, R. T. Oliver, and R. H. Reznik.** 2000. CT assessment of tumour response to treatment: comparison of linear, cross-sectional and volumetric measures of tumour size. *Br. J. Radiol.* **73**:1178–1184.
  21. **Solomon, J., S. Mavinkurve, D. Cox, and R. M. Summers.** 2004. Computer-assisted detection of subcutaneous melanomas: feasibility assessment. *Acad. Radiol.* **11**:678–685.
  22. **Solomon, J., K. Warren, E. Dombi, N. Patronas, and B. Widemann.** 2004. Automated detection and volume measurement of plexiform neurofibromas in neurofibromatosis 1 using magnetic resonance imaging. *Comput. Med. Imaging Graph.* **28**:257–265.
  23. **Stynen, D., J. Sarfati, A. Goris, M.-C. Prévost, M. Lesourd, H. Kamphuis, V. Darras, and J.-P. Latge.** 1992. Rat monoclonal antibodies against *Aspergillus* galactomannan. *Infect. Immun.* **60**:2237–2245.
  24. **Wald, A., W. Leisenring, J. A. van Burik, and R. A. Bowden.** 1997. Epidemiology of *Aspergillus* infections in a large cohort of patients undergoing bone marrow transplantation. *J. Infect. Dis.* **175**:1459–1466.
  25. **Walsh, T. J., J. Bacher, and P. A. Pizzo.** 1988. Chronic silastic central venous catheterization for induction, maintenance, and support of persistent granulocytopenia in rabbits. *Lab. Anim. Med.* **38**:467–470.
  26. **Walsh, T. J., K. Garrett, E. Feuerstein, M. Girton, M. Allende, J. Bacher, A. Francesconi, R. Schaufele, and P. A. Pizzo.** 1995. Therapeutic monitoring of experimental invasive pulmonary aspergillosis by ultrafast computerized tomography, a novel, noninvasive method for measuring responses to antifungal therapy. *Antimicrob. Agents Chemother.* **39**:1065–1069.
  27. **Walsh, T. J., J. L. Goodman, P. Pappas, I. Bekersky, D. N. Buell, M. Roden, J. Barrett, and E. J. Anaissie.** 2001. Safety, tolerance, and pharmacokinetics of high-dose liposomal amphotericin B (AmBisome) in patients infected with *Aspergillus* species and other filamentous fungi: maximum tolerated dose study. *Antimicrob. Agents Chemother.* **45**:3487–3496.
  28. **Walsh, T. J., C. McEntee, and D. M. Dixon.** 1987. Tissue homogenization with sterile reinforced polyethylene bags for quantitative culture of *Candida albicans*. *J. Clin. Microbiol.* **25**:931–932.